

Helicobacter pylori CagA inhibits PAR1-MARK family kinases by mimicking host substrates

Dragana Nešić¹, Marshall C Miller¹, Zachary T Quinkert², Markus Stein³, Brian T Chait² & C Erec Stebbins¹

The CagA protein of *Helicobacter pylori* interacts with numerous cellular factors and is associated with increased virulence and risk of gastric carcinoma. We present here the cocrystal structure of a subdomain of CagA with the human kinase PAR1b/MARK2, revealing that a CagA peptide mimics substrates of this kinase family, resembling eukaryotic protein kinase inhibitors. Mutagenesis of conserved residues central to this interaction renders CagA inactive as an inhibitor of MARK2.

Helicobacter pylori infects nearly 50% of the human population^{1,2} and has been closely linked to duodenal and gastric ulcers and adenocarcinomas¹. CagA is injected by *H. pylori* into the epithelial cells lining the stomach^{3–8}. Critical to many of the identified biological effects of the molecule on host cells is the so-called “repeats domain,” a region with a strain-specific number of contiguous repeats of a 30- to 40-residue segment containing the EPIYA amino acid motif⁷ (Fig. 1a). The repeats domain interacts with and inhibits the partition-defective and microtubule affinity-regulating kinase (PAR1-MARK) family of protein serine-threonine kinases^{9–11}.

To understand the mechanism of CagA inhibition of PAR1-MARK kinases, we determined the 2.2-Å crystal structure of MARK2 in complex with a subdomain of CagA spanning residues 885–1,005 of Western *H. pylori* strain 26695, which contains the A, B and C EPIYA repeats (Fig. 1a,b, Supplementary Table 1 and Supplementary Methods). Unexpectedly, the majority of this 120-residue CagA

domain was not visible in the crystals (although highly stable in complex with MARK2, and verified to be present by SDS-PAGE analysis of crystals; Supplementary Fig. 1a). In particular, the EPIYA motifs were disordered, and only a short 14-residue peptide possessed interpretable electron density (Fig. 1b and Supplementary Fig. 1b). The peptide does not adopt any clear secondary structure, but interacts with the kinase as an extended coil, burying ~950 Å² of surface area.

Two substantial differences are present between the unbound¹² and the CagA-bound forms of MARK2, and both are structural hallmarks of kinases in their fully activated state. The first difference is an overall hinge motion between the N- and C-terminal lobes of the kinase that brings them closer together in the presence of CagA (Supplementary Fig. 1c). This hinge motion is the same in each of the four independent copies of MARK2 in the asymmetric unit, making it unlikely that this is due to crystal packing. The second major difference is in the activation loop of the kinase, which adopts an ordered and activated structure in the presence of CagA^{13–16} (Fig. 1c), including the conformation of the canonical Asp-Phe-Gly (DFG) motif that is required for magnesium binding, and the position of a threonine (Thr208 in MARK2) that is phosphorylated

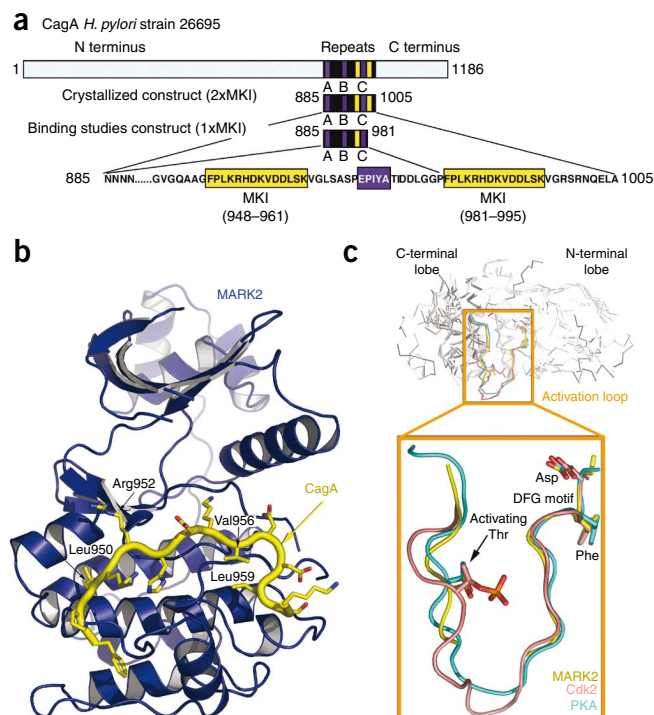


Figure 1 Overall structure of the CagA-MARK2 complex. (a) Schematic representation of CagA. The A, B and C EPIYA sequence repeats are shown as purple boxes. The crystallized construct (residues 885–1005) and the deletion mutant used in binding studies that lacked one of the MKI sequences (residues 885–981) are shown schematically as well. (b) Ribbon diagram of CagA-MARK2 complex, with MARK2 shown in blue and the ordered MARK2 inhibitory sequence (MKI (MARK2 kinase inhibitor), residues 948–961 and 982–995) in yellow. (c) Alignment of several protein kinases, focusing on the activation loop. Cdk2 (PDB 1JST (ref. 14)) and PKA (PDB 1ATP (refs. 15,16)) are from structures of the kinases in activated states (including Cdk2 bound to cyclin A with activating phosphorylation of threonine).

¹Laboratory of Structural Microbiology and ²Laboratory of Mass Spectrometry and Gaseous Ion Chemistry, Rockefeller University, New York, New York, USA.

³Department of Medical Microbiology and Immunology, University of Alberta, Edmonton, Alberta, Canada. Correspondence should be addressed to C.E.S. (stebbins@rockefeller.edu).

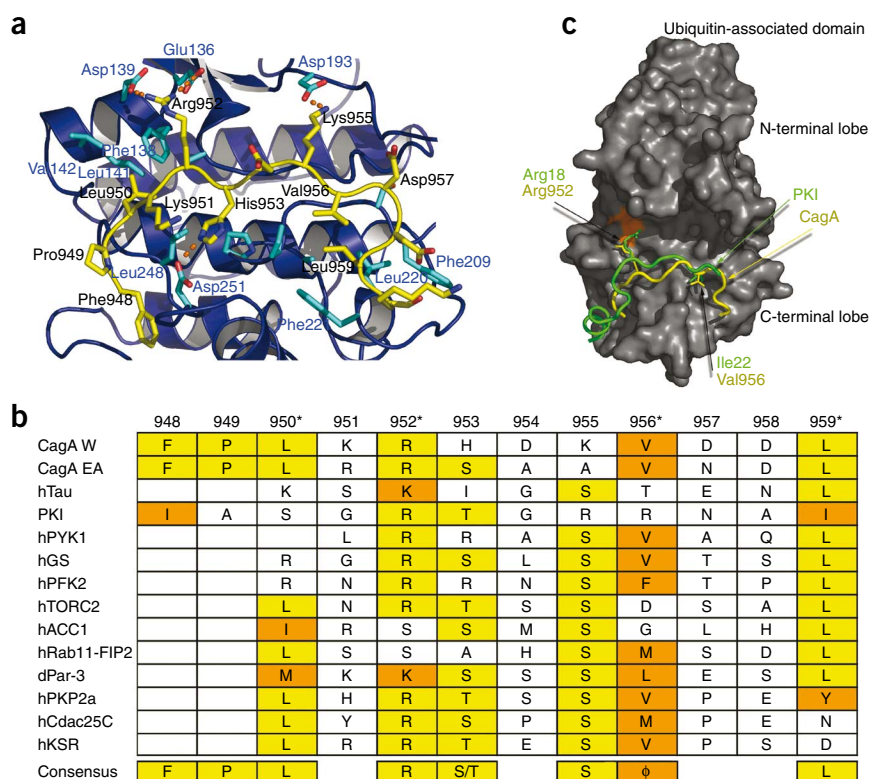


Figure 2 CagA is a pathogenic mimic of host substrates. (a) Details of the CagA peptide interaction. MARK2 is in blue with cyan side chains, and the MKI peptide of CagA is in yellow. (b) Alignment of PAR1-MARK and AMP-activated protein kinase (AMPK) family substrates with CagA peptide and, for comparison, PKI. Consensus identity is highlighted in yellow and conservation in orange. Φ indicates a hydrophobic consensus. Residues marked with asterisks anchor the CagA peptide to the MARK2 kinase. CagAW is CagA from *H. pylori* strain 26695 (Western subtype); CagA EA is the East Asian subtype of CagA. (c) Superposition of PKI and CagA obtained from aligning the kinases PKA and MARK2. The surface of MARK2 is shown in dark gray. Glu136 of MARK2, which forms a salt bridge with CagA Arg952, is shown in orange on the surface of MARK2.

of the kinase MARK2, we have termed “MKI” in analogy to PKI, which inhibits PKA (as discussed below).

Because the MKI sequence occurs twice in the crystallized construct, and because only the residues common to both repeats are visible, it was unclear from the crystal structure which of the two possible peptide regions (the first or second repeat of the MKI sequence) is binding. We addressed this issue through a combination of gel filtration

by activating kinases. These conformational states are remarkable for the fact that there is no nucleotide or magnesium present in the crystals, and no phosphorylation of Thr208.

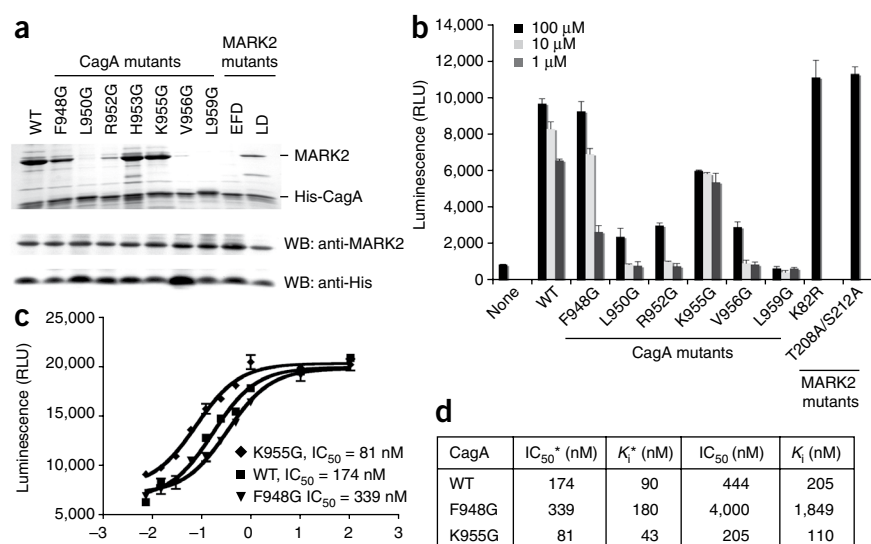
What makes this activated conformation of the kinase possible, even in the absence of several elements normally required, is the CagA peptide. The visible peptide spans the sequence FPLKRHDKVDLSK, a repeat motif occurring twice in the crystallized construct. This peptide, shown below to be sufficient for inhibition

chromatography and native MS. These results (**Supplementary Figs. 2–5** and **Supplementary Tables 2–4**) clearly showed that each MKI sequence is bound by a molecule of MARK2.

The MKI peptide of CagA occupies the substrate-binding site of the kinase that is located near the interface between the N- and C-terminal lobes of the enzyme, using several residues to mimic conserved features of the PAR1 and AMP-activated protein kinase family substrates (**Fig. 2a,b**). The peptide is anchored to the kinase

Figure 3 Mutational analysis of MKI mutants.

(a) Binding of wild-type or mutant hexahistidine-tagged CagA_{885–981} to wild-type or mutant MARK2_{39–364} was assayed by pull-down experiments on nickel–nitrilotriacetic acid–Sephacolumns. Eluted material was subjected to SDS-PAGE, and proteins were stained with Coomassie blue dye. Expression levels of MARK2 were determined by western blot of total cell extract with anti-MARK2 and anti-His for CagA expression. WT, wild type; EFD, MARK2 mutant (E136G, F138G, D139G); LD, MARK2 mutant (L248G, D251G). (b) Kinase activity of MARK2 in the presence of wild-type or mutant CagA synthetic MKI peptides using a luminescent kinase assay. tau-Peptide repeat 1 (TR1, NVKSKIGSTENLK) at 500 μM was used as a substrate with three different concentrations (100 μM, 10 μM and 1 μM) of CagA peptide inhibitors. MARK2 kinase-inactivated mutants K82R and T208A/S212A are negative controls. Error bars represent s.d. from the mean. (c) Determination of the half-maximal inhibitory concentration (IC₅₀) and K_i of CagA peptide inhibitors of MARK2 through a luminescence-based kinase assay. The TR1 peptide was used as substrate (150 μM in the experiments with previously activated MARK2, or 200 μM in experiments without prior activation of MARK2), with increasing concentration of inhibitory synthetic CagA peptides. Error bars represent s.d. from the mean. (d) Table summarizing IC₅₀ and K_i data. *-labeled values (IC₅₀* and K_i*) refer to kinase assays in which MARK2 was activated with MARK2-activating kinase (MARKK).



by four primary residues: Leu950, Arg952, Val956 and Leu959, numbering from the first repeat (Fig. 2a). Hydrophobic residues, especially leucine, are highly conserved at the corresponding positions in PAR1-MARK family kinase substrates (Fig. 2b), and the arginine at position 952 is also highly conserved. Several secondary interactions further stabilize the interaction: Phe948, His953 and Lys955, the latter positioning its terminal nitrogen atom in a location that mimics magnesium, forming hydrogen bonds with Asp193 of the MARK2 DFG motif (Fig. 2a). Overall, 7 out of 14 side chains in the peptide interact with the kinase.

Intriguingly, the manner in which the CagA MKI sequence binds in the substrate-binding cleft is reminiscent of the manner in which PKI binds to and inhibits PKA^{15,16} (Fig. 2c). A superposition of the two kinases bound to their respective inhibitors revealed that CagA residues 951–956 possess a main chain conformation overlapping with residues 17–22 of PKI, and the CagA residues bind in a very similar location with respect to PKI in PKA (Fig. 2c). In addition to these analogous locations and main chain conformations, several side chains of these kinase inhibitors interact with their targets in similar ways. For example, Arg18 of PKI is located very comparably to Arg952 of CagA (Fig. 2c), and both residues make hydrogen bonds with a conserved, nearly identically positioned glutamate in the two kinases (Glu127 in PKA, and Glu136 in MARK2). Both peptides also use a short hydrophobic residue at the position of CagA Val956 (Ile22 in PKI) to insert into a conserved hydrophobic pocket in the kinases (Fig. 2c).

To test the importance of these side chain interactions, a series of mutants were created in the MKI sequence of CagA. In order to prevent the second MKI sequence from biasing the results, these mutants were made in a construct in which one MKI site was deleted (the construct spanning residues 885–981; see Fig. 1a) as well as in synthetic peptides corresponding to the minimal region defined by the crystal structure. Hexahistidine-tagged CagA mutants were first examined for binding and coelution with untagged MARK2 from a nickel–nitrilotriacetic acid (Ni-NTA) resin (Fig. 3a). Point mutations of key anchoring residues, such as L950G and L959G, completely abolished binding to MARK2. The R952G mutant showed weak binding (Fig. 3a), but interaction was highly unstable, and the complex was disrupted by ion exchange chromatography. The mutation V956G almost completely eradicated binding to MARK2, highlighting the importance of this hydrophobic interaction with the kinase. We also created two MARK2 mutants, encompassing CagA-interacting residues E136G, F138G, and D139G in one construct (EFD) and L248G and D251G in the second (LD). The EFD mutations completely abolished interaction between MARK2 and CagA, consistent with their interactions with key CagA binding residues (Leu950 and Arg952), whereas the LD mutations did not.

Both basal MARK2 kinase activity (Fig. 3b) and MARKK (MARK2-activating kinase)-activated MARK2 (Fig. 3c) were tested *in vitro* in the presence of varying concentrations of short peptides containing the wild-type and mutant constructs of the MKI sequence. Synthetic peptides of CagA containing mutations in key interacting residues (Leu950, Arg952, Val956 or Leu959) failed to inhibit kinase activity

except at extremely high concentrations (100 μ M). In contrast, the wild-type peptide and the K955G mutant were very efficient inhibitors of MARK2. Intriguingly, the K955G peptide was a slightly more potent inhibitor of MARK2 than the wild-type peptide (Fig. 3c,d). Supporting this data, East Asian CagA subtypes contain glycine in the position that corresponds to Lys955 in Western CagA, and it has been reported that MARK2 binds more strongly to the East Asian CagA repeats region¹⁷.

This structure reveals that CagA mimics host substrates, using a short 14-residue peptide (MKI) to bind to the kinase substrate-binding site (see also **Supplementary Discussion** and **Supplementary Fig. 6**). Our biochemical experiments demonstrate that this peptide alone is sufficient to inhibit MARK2. In a dramatic example of convergent evolution, *H. pylori* has evolved a peptide to mimic host substrates of this kinase family in order to manipulate eukaryotic cellular biochemistry during infection.

Accession codes. Protein Data Bank: Coordinates for the CagA–MARK2 complex have been deposited with accession code 3IEC.

Note: Supplementary information is available on the Nature Structural & Molecular Biology website.

ACKNOWLEDGMENTS

We thank D. Oren and W. Shi for access to and assistance with crystallographic equipment. This work was funded in part by National Institutes of Health grants AI052182 (to C.E.S.) and RR00862, RR022220 (to B.T.C.), and by a Canadian Institutes of Health Research operating grant (MOP-62779) to M.S. M.S. is an Alberta Heritage Foundation for Medical Research Research Scholar.

AUTHOR CONTRIBUTIONS

D.N. performed all molecular biology, cloning, protein purification, functional assays, and crystallization; Z.T.Q. performed MS under the guidance of B.T.C.; M.C.M. collected crystallographic data along with D.N. and C.E.S. solved the structure. All authors contributed to writing the manuscript.

Published online at <http://www.nature.com/nsmb/>.

Reprints and permissions information is available online at <http://npg.nature.com/reprintsandpermissions/>.

1. Peek, R.M. Jr. & Blaser, M.J. *Nat. Rev. Cancer* **2**, 28–37 (2002).
2. Censini, S., Stein, M. & Covacci, A. *Curr. Opin. Microbiol.* **4**, 41–46 (2001).
3. Asahi, M. *et al. J. Exp. Med.* **191**, 593–602 (2000).
4. Backert, S. *et al. Cell. Microbiol.* **2**, 155–164 (2000).
5. Odenbreit, S. *et al. Science* **287**, 1497–1500 (2000).
6. Stein, M., Rappuoli, R. & Covacci, A. *Proc. Natl. Acad. Sci. USA* **97**, 1263–1268 (2000).
7. Covacci, A. *et al. Proc. Natl. Acad. Sci. USA* **90**, 5791–5795 (1993).
8. Tummuru, M.K., Cover, T.L. & Blaser, M.J. *Infect. Immun.* **61**, 1799–1809 (1993).
9. Saadat, I. *et al. Nature* **447**, 330–333 (2007).
10. Zeaiter, Z. *et al. Cell. Microbiol.* **10**, 781–794 (2008).
11. Higashi, H. *et al. Science* **295**, 683–686 (2002).
12. Panneerselvam, S., Marx, A., Mandelkow, E.M. & Mandelkow, E. *Structure* **14**, 173–183 (2006).
13. Huse, M. & Kuriyan, J. *Cell* **109**, 275–282 (2002).
14. Russo, A.A., Jeffrey, P.D. & Pavletich, N.P. *Nat. Struct. Biol.* **3**, 696–700 (1996).
15. Zheng, J. *et al. Acta Crystallogr. D Biol. Crystallogr.* **49**, 362–365 (1993).
16. Knighton, D.R. *et al. Science* **253**, 414–420 (1991).
17. Lu, H.S. *et al. Cancer Sci.* **99**, 2004–2011 (2008).